

MECHANICAL PROPERTIES OF CONCRETE DETERIORATED BY ALKALI  
AGGREGATE REACTION UNDER VARIOUS REINFORCEMENT RATIOS

W.Koyanagi, K.Rokugo and Y.Uchida  
Department of Civil Engineering,  
Gifu University.

Experimental studies were made mainly on the change of mechanical properties of reinforced concrete with or without AAR under the steel ratios of (0~2)%. Pulse velocity, dynamic Young's modulus, flexural and compressive behaviors were measured in addition to expansion and crack pattern. Deterioration due to AAR decreased as the steel ratio increased. The deterioration was remarkable when the steel ratio was less than 0.1% and not remarkable when it was more than 0.7%.

INTRODUCTION

Concrete deteriorates and mechanical properties of the concrete change when cracks due to alkali aggregate reaction (AAR) occur. In reinforced concrete structures, the degree of deterioration is influenced by the amount of the reinforcement ratio in the concrete, because the reinforcement restrains the expansion due to AAR. Various studies have been made and reported in the previous ICAAR. From the view point of structural design, however, further data must be accumulated on the influence of the deterioration due to AAR for structural behavior. Experimental works were made mainly on the change of mechanical properties of reinforced concrete with or without AAR and under various reinforcement ratios. Effect of the reinforcement ratios on the deterioration of concrete was studied.

EXPERIMENTAL PROCEDURES

Test Program

Concrete prism specimens with various reinforcement ratios were made. Specimen size was  $10 \times 10 \text{ cm}$  in cross section and  $100 \text{ cm}$  in length. A steel bar was placed at the center of the section. Two kinds of concrete (denoted as normal concrete and AAR concrete) with six levels of steel ratios (0 to 2%) were selected.

Specimens were cured in a fog room under  $43^\circ\text{C}$  for 38 weeks and expansion was measured for AAR concrete. After 38 weeks, crack patterns were observed and pulse velocity in each specimen was measured. Then, each specimen was cut into four pieces;  $40 \text{ cm}$ ,  $3 \times 20 \text{ cm}$ .

Dynamic Young's modulus and pulse velocity were measured for each 40cm specimen and then, flexural loading test was conducted for the specimen. For 20cm specimens, a compressive loading test was carried out after measuring pulse velocities. Normal concrete specimens were treated in the same way as AAR ones except for the curing condition and testing ages.

### Materials, Making and Curing

Ordinary portland cement was used. The alkali content of the cement was 0.61% ( $\text{Na}_2\text{O}$  equivalent). As to coarse aggregate, alkali reactive crushed stone (bronzite andesite:  $S_c = 180$ ,  $R_c = 124 \text{ mmol/l}$ , considered to be potentially deleterious) and non-reactive river gravel were used for AAR concrete. The maximum size of coarse aggregate was 20mm. River sand which seemed to be non-reactive was used. In order to accelerate the reaction,  $\text{Na}_2\text{SO}_3$  was added to concrete through mixing water to make the total alkali content to be 3% of cement content ( $\text{Na}_2\text{O}$  equivalent). For normal concrete, reactive aggregate and alkali additives were not used. Unit water and cement content were 176 and  $352 \text{ kg/m}^3$ , respectively. The ratio of reactive gravel to non-reactive was 4 : 6.

Five kinds of deformed steel bars were used, which had a nominal diameter of 3, 6, 10, 13 and 16mm. Yield (and tensile) strength of the bars were 34(49), 43(57), 39(55), 38(57) and 37(54)  $\text{kgf/mm}^2$ , respectively. The specimens were labeled by according to the rebar diameter. Reinforcement ratios  $p$  of the specimens were 0.07, 0.3, 0.7, 1.3 and 2%. Specimens without steel were also made and were called N ( $p = 0\%$ ).

In case of AAR concrete, specimens were demoulded at one day after casting. Two specimens were provided for each test condition. They were cured in a fog room of  $20^\circ\text{C}$  for about 4 weeks. Then, thermal cycles were given to the specimens in a wet condition. The first cycle was such that the room temperature was raised and kept at  $43^\circ\text{C}$  for 5 days and it turned to  $20^\circ\text{C}$  for 2 days and the cycle continued during 15 weeks. Then the period of the high temperature was extended to 30 to 35 days after the 15 weeks. Length changes of the specimens were measured at  $20^\circ\text{C}$ .

In case of normal concrete, specimens were also cured in a fog room at  $20^\circ\text{C}$  for 3 weeks. Temperature was not raised. The treatment of the specimen and the measuring methods were all the same as in case of AAR concrete except for the temperature and testing ages. Therefore, experimental procedures are explained only for AAR concrete, hereafter.

### Measurement

Length of the specimens was measured periodically with mechanical type strain gage (gage length: 250mm) at  $20^\circ\text{C}$ . Thirty eight weeks after high temperature curing, temperature was lowered to the room temperature. Then, crack width and crack patterns of the specimens were recorded.

Pulse velocity in longitudinal direction of each specimen was measured with ultra sonic tester. After the measurement, the specimens were cut into four pieces. The length of one piece was about 40cm and that of the other three pieces was about 20cm. Among the three 20cm specimens, only two were used for the next tests. Pulse velocity was also measured for the cut specimens. Dynamic Young's moduli were calculated for 40cm specimens from the

measured fundamental longitudinal frequencies.

Flexural tests were made for 40cm specimens through third point loading with 30cm span length. Deflection at each loading point was measured and load deflection diagrams were recorded. Cracking load was defined as the deflecting point from the initial straight portion in the diagram.

Compression tests were made by 20cm specimens. Both ends of the specimens were capped smoothly with gypsum. Wire strain gages were attached for each specimen and stress strain curves were measured.

## RESULTS AND DISCUSSIONS

### Expansion and Cracking

All the specimens expanded with time elapsed as shown in Fig. 1. Expansion decreased when the steel ratio increased. Amount of final expansion are 0.27% for N, 0.23% for D3, 0.15% for D6, 0.12% for D10, 0.10% for D13 and 0.08% for D16. Expansion for D3 was relatively larger than for the other cases and near to the case without reinforcement. Nominal steel stress is defined as the product of strain and Young's modulus. From the amount of expansion in the above, steel stress was considered to be attained to its yield stress in case of D3 specimen, whereas it seemed to be remained in elastic region for specimens with other kinds of reinforcement. In the early period, the room temperature did not reach to 40°C. It might affect the result that the expansion in this period was remained relatively small.

Cracks increased in their number and width with the time increased. Cracks tended to the axial direction when steel ratios increased, because the expansion in axial direction was restrained by the steel, whereas, that in perpendicular direction was not. Fig. 2 shows the crack pattern for N ( $p=0\%$ ) and for D16 ( $p=2\%$ ) as an example. Fig. 2 shows four faces in half length of the specimen. Maximum crack width was about 0.3 to 0.4mm for every specimen irrespective of steel ratio.

### Pulse Velocity and Young's Modulus

Fig. 3 shows the relationship of reinforcement ratio and pulse velocity. In Fig. 3(a), the results were obtained through 100cm specimen and in 3(b) through 20cm specimen. AR and NR indicate the results for AAR concrete and for normal concrete, respectively. Pulse velocity of AR was fairly smaller than that of NR when reinforcement ratio was small (in case of N and D3) and was almost the same when reinforcement ratio was large (more than D10) for 100cm specimen. When the reinforcement ratio increased pulse velocity increased because of the effect of reinforcement, which had higher Young's modulus. For shorter specimens the velocity became higher and the effect of AAR disappeared. The length of the pass seems to be longer the better in order to detect the deterioration due to AAR precisely from pulse velocity.

The relation between reinforcement ratio and dynamic Young's modulus  $E_d$  of normal and AAR concrete is shown in Fig. 4. In case of normal concrete,  $E_d$  remained almost constant irrespective of reinforcement ratio. In case of AAR concrete, however,  $E_d$  decreased

remarkably when the ratio was small, because the restriction to the expansion due to AAR was small. For the case without reinforcement, the ratio of  $E_d$  of AAR concrete to that of normal one is about 80%. The former was smaller than the latter when the reinforcement ratio was less than 1% and it agreed with the latter when the ratio was more than 1%.

The relation between reinforcement ratio and static Young's modulus  $E_s$  is given in Fig. 5.  $E_s$  for normal concrete increased slightly and proportionally to the increase of reinforcement.  $E_s$  of AAR concrete for the case without reinforcement was only 70% of that of normal concrete. The former agreed with the latter in the range where the reinforcement ratio was larger than 0.3%. The range where the effect of deterioration due to AAR appeared was wider in  $E_d$  than in  $E_s$ , though, for the case without reinforcement, the degree of the decrement was larger in  $E_s$  than in  $E_d$ .

### Flexural Behaviors

Load deflection diagrams under flexure for various reinforcement ratios are illustrated in Fig. 6a for AAR concrete and in Fig. 6b for normal concrete, respectively. The relation between reinforcement ratio to cracking load and that to the deflection at the cracking load are shown in Figs. 7 and 8, respectively, for both AAR concrete and normal one. The similar relation between reinforcement ratio to ultimate strength is given in Fig. 9.

Cracking load for normal concrete was almost constant regardless of reinforcement ratio, while that for AAR concrete depended highly on the ratio. In case without reinforcement, deteriorated beam specimens broke easily and cracking load for AAR concrete was as low as 60% of that for normal concrete. However, cracking load of AAR concrete increased with the increase of reinforcement ratio and it became larger than that of normal concrete when the ratio becomes more than 0.1%. When the ratio is 2% it became twice as large as the normal one. This seems to be caused by the internal compressive stress which was induced as a reaction force by the restraint of expansion due to AAR by the reinforcement. Deflections at the cracking loads for AAR concrete were several times larger than that for normal concrete. This means that the rigidity of AAR concrete was smaller than that of normal concrete, even though, the cracking load was higher.

The maximum flexural load for N and D3 for AAR concrete specimens were the same as their cracking load and, consequently, they were smaller than that for normal concrete one, as stated before. In the range where the ratio was more than 0.7%, ultimate flexural strength of AAR concrete specimens was the same or slightly larger to that for normal one.

### CONCLUSIONS

Experimental studies were made on the effect of the amount of reinforcement on the degree of deterioration of mechanical properties of concrete due to AAR. Principal conclusions derived from the study are summarized as follows.

- (1) Expansion of concrete due to AAR was restrained by reinforcement and the restraining effect became higher with the increase of reinforcement ratio. When the reinforcing steel yielded the effect remained low.

- (2) Pulse velocity decreased because of AAR when reinforcement ratio was relatively small. However, it remained almost the same when the ratio was more than 0.7%. Accuracy of detection of the deterioration changed according to the measuring length of the pulse velocity. When the length was 20cm, the deterioration due to AAR was not be detected.
- (3) Effect of deterioration due to AAR appeared also in Young's moduli  $E_d$  and  $E_s$ , in a range of the small reinforcement ratio. The range of reinforcement ratio where Young's modulus of AAR concrete was less than that of normal concrete was wider in  $E_d$  than in  $E_s$ , though, the decrement of  $E_s$  was larger than that of  $E_d$  for the case without reinforcement.
- (4) Flexural cracking load of normal concrete was almost the same regardless of reinforcement ratio, while that of AAR concrete depended highly on the ratio. Cracking load of AAR concrete increased with the increase of the ratio and it became larger than that of normal concrete when the ratio became more than 0.1%. This seemed to be caused by the internal compressive stress which was induced as a reaction force by the restraint of expansion due to AAR.
- (5) Displacement at the cracking load for AAR concrete was several times larger than that for normal concrete. This means that the flexural rigidity of AAR concrete was smaller than that of normal concrete, even though the cracking load was higher.
- (6) In the case of AAR concrete with small reinforcement ratio, the maximum flexural loads were the same as their cracking load and, consequently, they were smaller than that for normal concrete. In the range where the ratio was more than 0.7%, ultimate flexural strength of AAR concrete specimens was slightly higher than that for normal concrete specimens.
- (7) The deterioration of the mechanical properties due to AAR was remarkable when the reinforcement ratio was less than 0.1% and not remarkable when it was more than 0.7%.

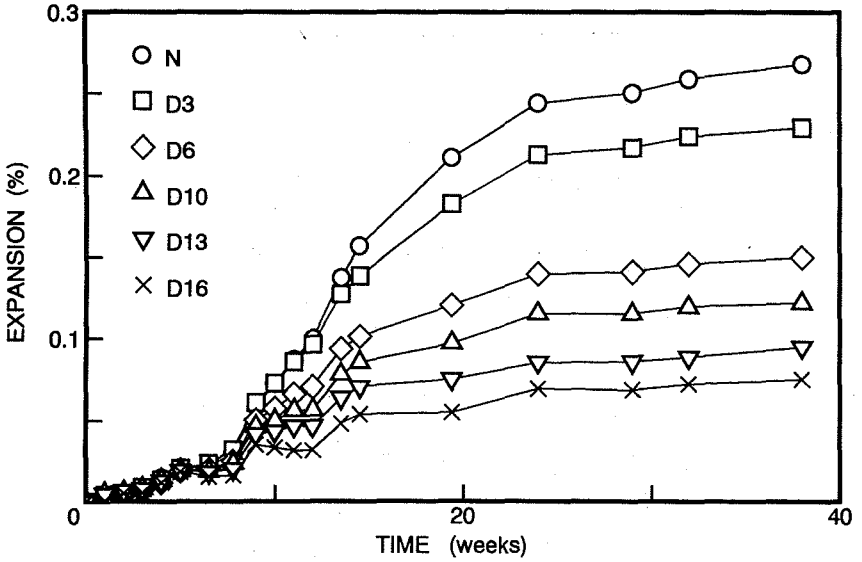
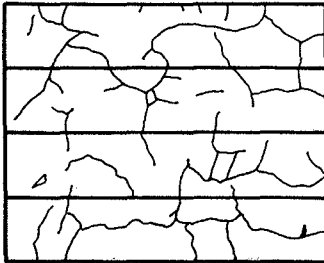
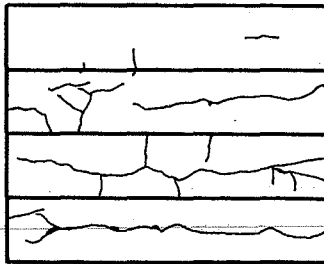


Fig. 1 Effect of Reinforcement on Expansion

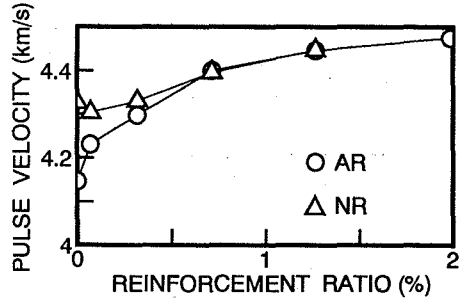


(a) AR-N

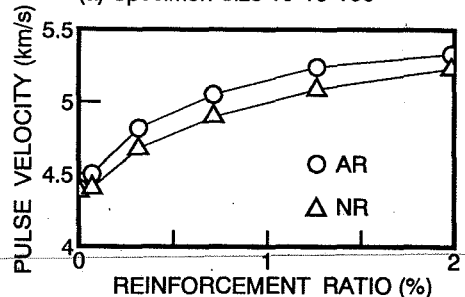


(b) AR-D16

Fig. 2 Crack Pattern



(a) Specimen Size 10\*10\*100



(b) Specimen Size 10\*10\*20

Fig. 3 Pulse Velocity

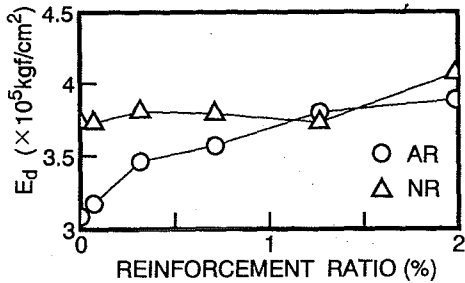


Fig. 4 Dynamic Young's Modulus  $E_d$

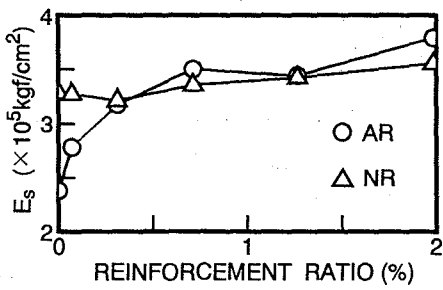


Fig. 5 Static Young's Modulus  $E_s$

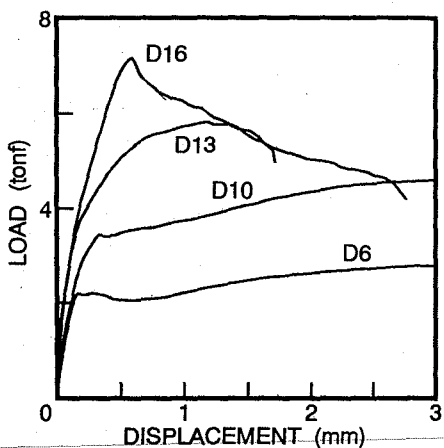


Fig. 6a Load-Displacement Curve (AR)

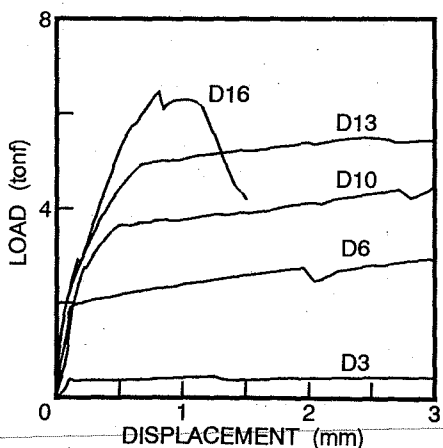


Fig. 6b Load-Displacement Curve (NR)

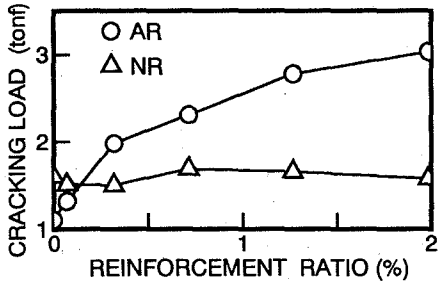


Fig. 7 Cracking Load

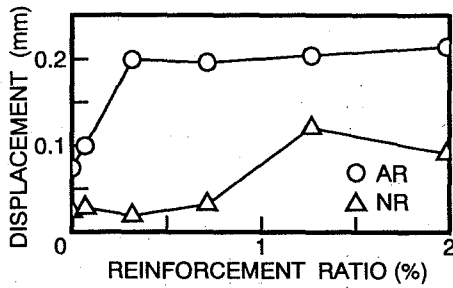


Fig. 8 Displacement at Cracking Load

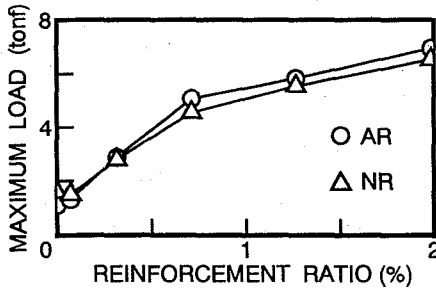


Fig. 9 Maximum Load